Inorganic Chemistry

Article

pubs.acs.org/IC

Soluble Diamagnetic Model for Malaria Pigment: Coordination Chemistry of Gallium(III)protoporphyrin-IX

D. Scott Bohle,*[,†] Erin L. Dodd,[†] Tyler B. J. Pinter,[‡] and Martin J. Stillman[‡]

[†]Department of Chemistry, McGill University, Montreal, Quebec, Canada

[‡]Department of Chemistry, The University of Western Ontario, London, Ontario, Canada

ABSTRACT: The facile axial ligand exchange properties of gallium(III) protoporphyrin IX in methanol solution were utilized to explore self-association interactions by NMR techniques. Structural changes were observed, as well as competitive behavior with the ligands acetate and fluoride, which differed from that seen with the synthetic analogue gallium(III) octaethylporphyrin which lacks acid groups in its side-chains and has less solution heterogeneity as indicated by absorption and MCD spectroscopies. The propionic acid side chains of protoporphyrin IX are implicated in all such interactions of PPIX, and both dynamic metal-propionic interactions and the formation of propionate-bridged dimers are observed. Fluoride coordination provides an unusual example of slow ligand exchange, and this allows for the identification of a fluoride bridged dimer in solution. An improved synthesis of the chloride and hydroxide complexes of gallium(III) protoporphyrin IX is reported. An insoluble gallium analogue of hematin anhydride is described. In general, the interactions between solvent and the metal are found to confer very high solubility, making [Ga(PPIX)]$^+$ a useful model for ferric heme species.

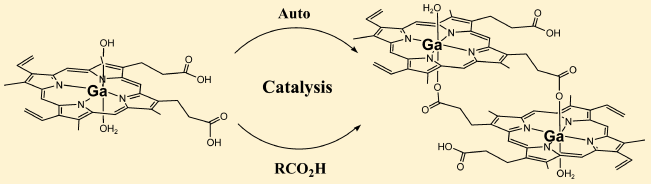

INTRODUCTION

Malaria continues to be a global problem annually killing hundreds of thousands, many of them children, despite advances in treatment and preventative measures.[1,2] In the face of rising global resistance in Plasmodium *falciparum* to artemisinin-based combination therapies, it is important that we develop a thorough understanding of the drugs we currently have. Among the most useful drugs are the quinoline family of antimalarials[3,4] which inhibit the biocrystallization of hemozoin by the parasite, the mechanism of formation of which is yet unknown and the subject of much debate.[5−7] Although resistance to these antimalarials is now pervasive, the mechanism of hemozoin formation and the mechanism of drug action remain the same.

Hemozoin, or hematin anhydride, is a byproduct of hemoglobin digestion in the digestive vacuole of the malaria parasite. It has been determined to be a highly crystalline form of dimerized heme. The structure of the synthetic dimer was determined from powder diffraction using synchrotron radiation[8] (Figure 1) and is composed of propionate-bridged dimeric units intermolecularly linked through hydrogen bonding between the free propionic acid groups.[9] Once formed, crystalline hematin anhydride is almost entirely insoluble in any solvent and dissolves with reaction only in strong acids or under reducing conditions with mercaptans.

The orientation of heme dimer units of the hematin anhydride gives rise to this stability and is necessarily a product of the solution behavior of the free heme and its surroundings both in vivo and in vitro during the biocrystallization process. In an effort to find a new probe for this ill-defined system, we have developed an analogous system using gallium(III) protoporphyrin IX species. We recently reported optical spectroscopy and myoglobin binding of Ga(PPIX)[10] as well as a dimer structure in which the interdimer hydrogen bond linkages were absent, leading to a compound with high solubility and axial lability.[11] In this paper, we lay the foundation for our modeling studies through a series of experiments which explore the complex exchange chemistry of these protoporphyrin derivatives in solution.

Gallium(III) protoporphyrin IX (Ga(PPIX)(X), where X is chloride, Cl^-, or hydroxide, OH^-) is diamagnetic and fluorescent, and highly soluble in methanol and pyridine, and somewhat so in similar organic solvents. The paramagnetism of the high spin iron(III) of hematin anhydride itself and its precursors has made it difficult to obtain detailed quantitative NMR information as the signal is weak, broad, and shifted. This, combined with the insolubility of the compound, makes NMR analysis of naturally occurring free heme species doubly troublesome. Gallium(III) is an ideal substitute for iron(III) because the ions have the same charge, approximately the same ionic radius (0.62 Å vs 0.65 Å),[12] and similar coordination preferences. However, gallium(III) has a filled d shell and is diamagnetic, and therefore complexes of gallium(III) are ideal for study by NMR. Most importantly, protoporphyrin IX complexes of gallium(III) are highly soluble in certain solvents. Preparation of Ga(III) synthetic porphyrin derivatives and their properties,[13] particularly photophysical properties[14] are well described in the literature, and a few natural porphyrin derivatives have been described[15] as well as synthetic dimers and trimers.[16] Compounds with both anionic[13,14,17−21] and organometallic[22−24] axial ligands have been described. In particular, ^{1}H NMR is of

Received: May 25, 2012
Published: October 2, 2012

dx.doi.org/10.1021/ic301106g | *Inorg. Chem.* 2012, 51, 10747−10761

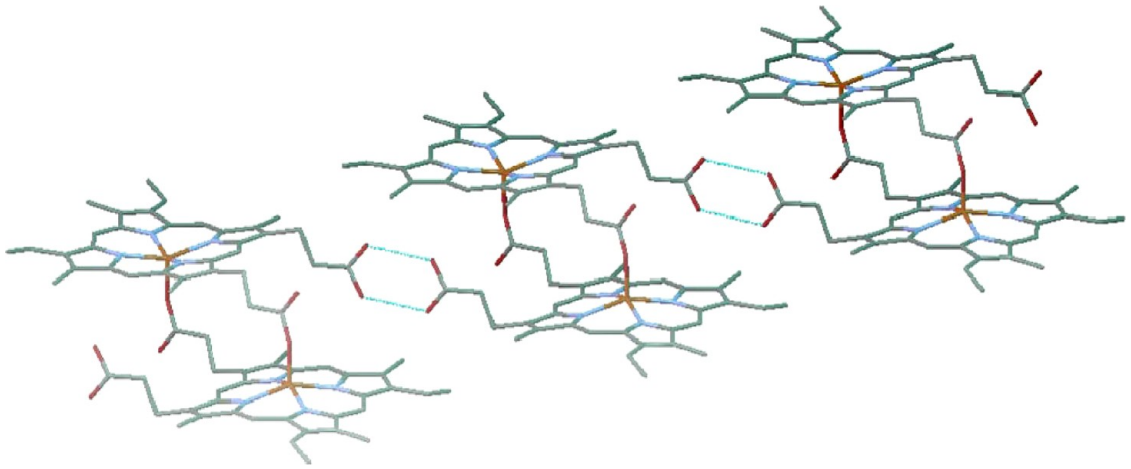

Figure 1. Structure of hematin anhydride determined unambiguously by powder diffraction, spacegroup $P\bar{1}$.[8]

interest because of the sensitivity of this technique to perturbations of short-range chemical environments. Protons, being on the edges of the molecules in question, are inherently more sensitive to the interactions at the periphery of the molecule.

It became evident early on in the work that the Ga(PPIX)(X) (X = Cl, OH) was interacting with both itself and with solvent in solution, and that its solubility was dependent on solvent interactions which made aggregation of the sort to which metalloprotoporphyrin IX compounds are prone far less favorable. Ga(PPIX)(OH) is only soluble in coordinating solvents, and only moderately soluble in noncoordinating solvents in the presence of ligands such as pyridine and pyrrolidine. The latter has been used to minimize aggregation effects in zinc(II) protoporphyrin IX dimethyl ester solutions.[25] These effects must be characterized to make use of the solubility and ease of handling of Ga(PPIX)(OH) in heme-modeling studies. The work of Abraham and co-workers[25,26] in the 1970s proposed mechanisms for aggregation for diamagnetic M(II) protoporphyrin IX methyl esters. It is necessary to tackle the more complicated question of M(III) protoporphyrin IX with free acid groups to truly address the biological relevance of the model. The nature of these interactions is of significant interest as it provides some of the most clear and concise evidence for how the behavior of M(III) protoporphyrin IX in solution is mediated and directed by the propionic acid side chains. This has far-reaching implications for how we understand the solution behavior of heme itself, and provides direct evidence that the propionic acid groups play an active role in the chemistry of free heme. Here we describe an improved synthetic method used to synthesize gallium(III) protoporphyrin IX. This synthetic method is adapted from the base-mediated synthesis of gallium(III) protoporphyrin IX hydroxide hydrate Ga(PPIX)(OH)(OH_2) reported[15] by Nakae et al. We describe its complete characterization, and highlight work done to understand self-interaction behavior in solution as it pertains to the biological questions we wish to answer with this model system.

The self-interactions and solvent interactions of Ga(PPIX)(X) (X = Cl, OH) were probed by NMR. Experiments were repeated using synthetic octaethylporphyrin (OEP) analogues Ga(OEP)Cl and Ga(OEP)OH for comparison. These compounds were synthesized in excellent (85%) yields using the same methods used for the protoporphyrin IX species. An important aim of our work has been to use ^{1}H NMR to characterize the interaction between our heme model and its surroundings and follow axial ligand reactivity.[27] We also report the synthesis of a gallium(III) protoporphyrin IX propionate-bridged reciprocal dimer [Ga(PPIX)]$_2$ analogous to hematin anhydride using modifications of the acid-catalyzed hematin anhydride synthesis.[28] Reciprocal dimerization is proposed to be favored over dimerization through a single metal−oxygen bond in methanol solution because of lability at the metal, simple proximity, and the chelate effect. The solution MCD and absorption spectroscopy of Ga(OEP)(OMe) are contrasted with related systems.

EXPERIMENTAL SECTION

Octaethylporphine and protoporphyrin IX dimethyl ester were purchased from Frontier Scientific, Inc. Gallium trichloride was purchased from STREM chemicals. All other reagents were purchased from Sigma-Aldrich and used without further purification. HPLC-grade methanol, HPLC-grade dichloromethane, and double-distilled 2,6-lutidine were purchased from Sigma-Aldrich and used without further purification. NMR-grade d_4-methanol was purchased from Cambridge Isotopes and used without further purification. All single ^{1}H, NOESY, variable temperature and ^{1}H titration NMR experiments were performed on a 500 MHz Varian Mercury NMR spectrometer. Differential scanning calorimetry measurements were performed on a TA Instruments DSC 2010. Infrared spectroscopy was performed on an ABB Bomem MB series IR spectrometer. NMR spectra were analyzed using MestreNOVA software. Equilibrium constants were determined using WinEQNMR2.[29] The equilibrium constants are attributed to dimerization reactions, because the low concentrations employed and the almost unitary values found in the analysis correspond to minimal higher oligomerization. In addition, the concentration dependent experiments suggest little cooperativity which would result from more highly favorable oligomerization. Elemental analysis was performed with the help of the elemental analysis service at the chemistry department of the University of Montreal.

CD spectra were measured on a Jasco 815 spectropolarimeter (Jasco, New Jersey), and MCD spectra were recorded by adding a 1.4 T permanent magnet (OLIS, U.S.A.) (acquisition = 3 scans; $T_{cell} \sim 295$ K). Scan parameters were as follows: step scan; range 700−250 nm; data pitch = 1 nm; bandwidth = 0.5 nm; response = 1 s. MCD spectra were corrected for the zero field CD spectrum and zeroed at 700 nm before a 3 point fast Fourier transform filter was applied to smooth the data.

ESI-MS Data. A Bruker micrOTOF II ESI-TOF mass spectrometer (Bruker, Canada) operated in the positive ion mode was used for all electrospray ionization mass spectrometry (ESI-MS) measurements. Samples were infused into the spectrometer at a rate of 300 $\mu L \cdot h^{-1}$ using a microliter infusion pump. The instrument was calibrated with an external NaI/CsI standard solution. Data were processed using the Bruker DataAnalysis 4.0 software. Parameters: rolling average = 2 × 0.5 Hz; end plate offset = −500 V; nebulizer = 2.0 bar; dry gas

temp = 473 K; flow rate = 6.0 L/min; capillary voltage = 4500 V; capillary exit = 225 V; skimmer 1 = 42 V; hexapole = 23.0 V; hexapole RF = 425 Vpp.

Density Functional Theory (DFT) and Time-Dependent DFT (TD-DFT) Calculations. The Ga-OEP crystal structure coordinates were used as the starting point geometry for calculations. The structure underwent low level DFT (B88-PW91) geometry optimization using Scigress (Fujitsu America). Further ground state geometry optimizations were carried out with the Gaussian 03 program[30] by higher-level B3LYP/6-31G DFT calculations. The TD-DFT calculation for this optimized ground state geometry was then carried out as a separate experiment in Gaussian 03. The absence of Ga parametrization for DFT calculations required the use of a gallium pseudopotential (LANL2DZ "valence basis + pseudopotential" (https://bse.pnl.gov/bse/portal).[31,32]

Synthesis. *Preparation of Ga(PPIX)Cl (**1**).* Protoporphyrin IX dimethyl ester (0.85 mmol) was suspended in 2,6-lutidine (20 mL). In a glovebag assembly under nitrogen atmosphere, gallium trichloride (28 mmol) was dissolved in 2,6-lutidine (10 mL), and added dropwise to the protoporphyrin IX dimethyl ester under a stream of nitrogen. 2,6-Lutidine was added to increase the volume to 50 mL. The reaction mixture was heated at 150 °C for 1.5 h, then cooled, diluted with 500 mL of concentrated brine, then acidified to pH = 4 with 20% aqueous citric acid, and the purple precipitate was collected by filtration and washed with distilled water (3 × 100 mL). The solid collected was dissolved in methanol (75 mL) and washed though the frit. Solvent was evaporated and solid dried in vacuo to yield purple-red solid in 85% yield. UV/vis λ_{max} (MeOH, path length 0.4 cm): A_{max} [nm] (ε (L mol^{-1} cm^{-1})): 405 (309 000), 539 (16 200), 577 (20 100). IR (KBr) (cm^{-1}): 1715 and 1626 ($\nu(CO_2)_{sym}$), 1383 ($\nu(CO_2)_{asym}$). ^{1}H NMR: (0.18 M in d$_4$-methanol, referenced to TMS), 500 MHz) $\delta(ppm)$: 3.23 (propionic acid $H_{2\beta}$ and $H_{18\beta}$, 4H, b), 3.78 (methyl $H_{3\alpha}$, 3H, s), 3.81 (methyl $H_{17\alpha}$, 3H, s), 3.87 (methyl $H_{8\alpha}$, 3H, s), 3.89 (methyl $H_{12\alpha}$, 3H, s), 4.55 (propionic acid $H_{2\alpha}$ and $_{18\alpha}$, 4H, b), 6.34 (vinyl $H_{7\beta}$ trans to porphyrin, 1H, d, $^3J_{7\alpha\text{-}7\beta(trans)}$ = 11.5 Hz), 6.35 (vinyl $H_{12\beta}$ trans to porphyrin,1H, d, $^3J_{12\alpha\text{-}12\beta(trans)}$ = 11.5 Hz), 6.49 (vinyl $H_{7\beta}$ cis to porphyrin, 1H, $^3J_{7\alpha\text{-}7\beta(cis)}$ = 17.8 Hz), 6.51 (vinyl $H_{12\beta}$ cis to porphyrin, 1H, $^3J_{12\alpha\text{-}12\beta(cis)}$ = 17.8 Hz), 8.54 (vinyl $H_{7\alpha}$, 1H, dd, $^3J_{7\alpha\text{-}7\beta(cis)}$ = 17.8 Hz, $^3J_{7\alpha\text{-}7\beta(trans)}$ = 11.5 Hz), 8.56 (vinyl $H_{12\alpha}$, 1H, dd, $^3J_{12\alpha\text{-}12\beta(cis)}$ = 17.8 Hz, $^3J_{12\alpha\text{-}12\beta(trans)}$ = 11.5 Hz), 10.60 (methine H_{15}, 1H, s), 10.61 (methine H_5, 1H, s), 10.67 (methine H_{20}, 1H, b), 10.68 (methine H_{10}, 1H, s). Elemental analysis: found (expected): C, 61.22 (61.33); H, 5.12 (4.84); N, 8.02 (8.41)

*Preparation of Ga(PPIX)(OH) (**2**).* Gallium(III) protoporphyrin IX chloride (0.45 mmol) was dissolved in 50 mL of methanol. KOH in methanol (100 mL, 2.2 M) was added to this solution which was stirred for 1 h at room temperature, then acidified to pH = 4 with 20% aqueous citric acid, diluted to over 600 mL with concentrated brine and filtered. The solid collected was redissolved in 75 mL of methanol and washed though the frit. Ga(PPIX)(OH) is obtained upon evaporation of solvent and dried in vacuo. Yield was 85%. The following spectroscopic data agree with all of those reported by Nakae et al.[15] UV/vis λ_{max} (MeOH, path length 0.4 cm): A_{max} [nm] (ε (L mol^{-1} cm^{-1})): 405 (282 000), 539 (18 800), 577 (15 400). IR (KBr) (cm^{-1}): 1725 and 1628 ($\nu(CO_2)_{sym}$), 1378 ($\nu(CO_2)_{asym}$) ^{1}H NMR: (0.18 M in d$_4$-methanol, referenced to TMS), 500 MHz) $\delta(ppm)$: 3.22 (propionic acid $H_{2\beta}$ and $H_{18\beta}$, 4H, b), 3.76 (methyl $H_{3\alpha}$, 3H, s), 3.79 (methyl $H_{17\alpha}$, 3H, s), 3.87 (methyl $H_{8\alpha}$, 3H, s), 3.89 (methyl $H_{12\alpha}$, 3H, s), 4.52 (propionic acid $H_{2\alpha}$ and $_{18\alpha}$, 4H, b), 6.34 (vinyl $H_{7\beta}$ trans to porphyrin, 1H, d, $^3J_{7\alpha\text{-}7\beta(trans)}$ = 11.6 Hz), 6.35 (vinyl $H_{12\beta}$ trans to porphyrin,1H, d, $^3J_{12\alpha\text{-}12\beta(trans)}$ = 11.6 Hz), 6.49 (vinyl $H_{7\beta}$ cis to porphyrin, 1H, $^3J_{7\alpha\text{-}7\beta(cis)}$ = 17.9 Hz), 6.50 (vinyl $H_{12\beta}$ cis to porphyrin, 1H, $^3J_{12\alpha\text{-}12\beta(cis)}$ = 17.9 Hz), 8.54 (vinyl $H_{7\alpha}$, 1H, dd, $^3J_{7\alpha\text{-}7\beta(cis)}$ = 17.9 Hz, $^3J_{7\alpha\text{-}7\beta(trans)}$ = 11.6 Hz), 8.56 (vinyl $H_{12\alpha}$, 1H, dd, $^3J_{12\alpha\text{-}12\beta(cis)}$ = 17.9 Hz, $^3J_{12\alpha\text{-}12\beta(trans)}$ = 11.6 Hz), 10.59 (methine H_{15}, 1H, s), 10.60 (methine H_5, 1H, s), 10.67 (methine H_{20}, 1H, b), 10.74 (methine H_{10}, 1H, s). Elemental analysis: found: C, 61.88; H, 5.10; N, 8.24; expected if Ga(PPIX)(OH): C, 63.08; H, 5.14; N, 8.65; expected if Ga(PPIX)(OH)(H_2O): C, 61.37; H, 5.30; N, 8.42.

*Preparation of [Ga(PPIX)]$_2$ (**3**).* Gallium(III) protoporphyrin IX hydroxide (0.15 mmol) was dissolved in aqueous sodium hydroxide solution (1 M, 75 mL) and stirred for 30 min. The solution was degassed by bubbling nitrogen gas through while stirring for 30 min. Propionic acid (4 mL) was added dropwise over 20 min using a syringe pump. The pH of the solution was 4 at the end of the addition. The mixture was heated to 70 °C and annealed at this temperature without stirring for 8 days. The solid precipitate was collected by centrifugation and washed with water and aqueous sodium bicarbonate solution (0.01 M), discarding the decanted liquid. The washing step was repeated three times. Solid residue was dried in vacuo. IR (KBr) (cm^{-1}): 1713 and 1665 ($\nu(CO_2)_{sym}$), 1223 ($\nu(CO_2)_{asym}$)

*Preparation of Ga(OEP)Cl (**4**).* Octaethylporphine (0.47 mmol) was suspended in 2,6-lutidine (10 mL). In a glovebag assembly under nitrogen, gallium trichloride (17 mmol) was dissolved in 2,6-lutidine (10 mL) under nitrogen atmosphere, and added dropwise to the porphyrin under a stream of nitrogen. The reaction mixture was refluxed at 150 °C for 1.5 h then cooled, diluted with 500 mL of distilled water and filtered, washing with distilled water. The dry solid collected was redissolved in 75 mL of dichloromethane and washed though the frit. Ga(OEP)Cl is obtained upon immediate evaporation of solvent at room temperature in vacuo. ^{1}H NMR: (0.18 M in d$_4$-methanol, referenced to TMS), 500 MHz) $\delta(ppm)$: 1.84 (CH_3, 24H, t, J^3 = 7.62 Hz), 3.92 (CH_2, 16H, quar, J^3 = 7.62 Hz), 9.87 (CH, 4H, s). Elemental analysis: found (expected) C, 67.48 (67.78); H, 7.40 (6.95); N, 8.55 (8.78). Spectroscopically identical to literature report.[14]

*Preparation of Ga(OEP)(OH) (**5**).* Gallium(III) octaethylporphyrin chloride (0.47 mmol) was dissolved in methanol (50 mL). KOH in methanol (100 mL, 2.2 M) was added to this solution which was stirred for 1 h at room temperature, then acidified to pH = 4 with 20% aqueous citric acid, diluted to over 600 mL with distilled water and filtered. The dry solid collected was redissolved in 75 mL of dichloromethane and washed though the frit. Ga(OEP)(OH) is obtained upon evaporation of solvent . ^{1}H NMR: (0.18 M in d$_4$-methanol), 500 MHz) $\delta(ppm)$: 1.82 (CH_3, 24H, t, J^3 = 7.67 Hz), 3.88 (CH_2, 16H, quar, J^3 = 7.67 Hz), 9.80 (CH, 4H, s). Elemental analysis: found: C, 70.03; H, 7.56; N, 8.78; expected if Ga(OEP)(OH): C, 69.80; H, 7.32; N, 9.04; expected if Ga(OEP)(OH)(H_2O): C, 67.82; H, 7.43; N, 8.79. Spectroscopically identical to literature report.[13]

*Preparation of Ga(OEP)(OMe) (**6**).* Gallium(III) octaethylporphyrin chloride (500 mg) was dissolved in methanol (100 mL) and left sitting for 24 h. Solvent was removed in vacuo at 60 °C, and the solid residue left under vacuum overnight. Elemental analysis: found (expected) C, 69.60 (70.15); H, 7.42 (7.48); N, 8.77 (8.84). Spectroscopically identical to literature report.[13]

Methods. *NMR Titration of Ga(PPIX)(X) (X = Cl, OH) against Ligand Source (Acetic Acid) or Base (Tetramethylammonium Hydroxide).* All volume measurements performed using Hamilton gastight syringes for accuracy. A solution of 1 M of the compound(s) to be titrated is prepared in d$_4$-methanol (200 μL). Separately, Ga(PPIX)(X) (5 nmol) is dissolved in d$_4$-methanol (500 μL) in an NMR tube. Dichloromethane (2.5 μL, HPLC-grade) is added as an internal standard. Aliquots of titrant solution were added to the sample in the NMR tube over the course of the titration, with ^{1}H NMR spectra taken after 20 inversions to obtain homogeneity initially and again upon each addition. The Ga(PPIX)(X) sample must be freshly made, kept dark, prepared immediately before use, and used quickly, as some aggregation occurs over the first few hours at this concentration.

NMR Titration of Ga(PPIX)(X), Ga(OEP)Cl (X = Cl, OH) against Base. Titration was performed just as the titration described above, but with aliquots of a solution of 25% tetramethylammonium hydroxide in methanol (as bought with no further preparation) added as titrant.

NMR Dilution of Ga(PPIX)(X), Ga(OEP)Cl (X = Cl, OH). Dilution was performed just as the titration described above, but with aliquots of pure d$_4$-methanol added as titrant.

NMR Titration of Ga(PPIX)(X), Ga(OEP)Cl (X = Cl, OH) against Fluoride Source. The fluoride source was NBu_4F or CsF. Titrations were performed as above. In addition, ^{19}F spectra were obtained for samples at the beginning of titration, at 1:1 ratio, and after addition of

large excess of the fluoride source. 2D COSY and NOESY spectra were obtained at each of these points.

Low Temperature NMR. Ga(PPIX)(OH) (5 nmol) is dissolved in d_4-methanol (500 μL). CH_2Cl_2 (2.5 μL) was added as an internal standard to confirm concentrations. The instrument was cooled from +25 °C to −75 °C with ^{1}H NMR spectra taken at each 10 °C interval, allowing 30 min equilibration time for each sample to minimize thermal gradient currents in the sample. The instrument was tuned and shimmed at each temperature interval.

RESULTS AND DISCUSSION

The solubility of gallium complexes of the natural porphyrin protoporphyrin IX gives access to a wealth of structural information. The axial ligand positions are labile in solution,[13] and this reactivity is readily followed by NMR spectroscopy. Titrations were carried out with both protoporphyrin IX and octaethylporphyrin moieties against the anionic ligands acetate (AcO^-) and fluoride (F^-) to further explore the reactivity at the Ga(III) metal center through the structural changes observed via changes in chemical shift. The differences observed between the synthetic and the natural porphyrins allow us to differentiate between effects mediated by protoporphyrin IX substituents and those that involve only the metal. The shifts in the ^{1}H NMR spectrum which accompany ligand exchange range from subtle, as with acetate, to quite dramatic in the case of fluoride and upon deprotonation of the propionic acid groups of the porphyrin ring. The NMR peak position is found to be strongly dependent on interactions with the side chains of the porphyrin as emphasized by differences in behavior between Ga(PPIX) species and Ga(OEP) species which lack reactive side chains. The titration results of Ga(OEP)X and acetic acid indicate that the dimerization is favored over solvolysis. This in turn allows us to accurately determine the equilibrium constants and composition in a multiequilibrium system in fast exchange by NMR spectroscopy, even for this underdetermined system. In general these substitution reactions are also dehydration reactions and are acid-catalyzed. Thus the name "anhydride" is used in describing the hematin anhydride structure in Figure 1. For the bis-propionic acid substituted protoporphyrin-IX system the pH regimes corresponding to a single protonation can also catalyze, and therefore autocatalyze, the substitution reactions at the metal.

To obtain the materials necessary to perform these trials, we made some improvements upon the synthesis of the starting materials Ga(PPIX)(Cl) and Ga(PPIX)(OH) to consistently ensure purity and high yields. This is necessary particularly

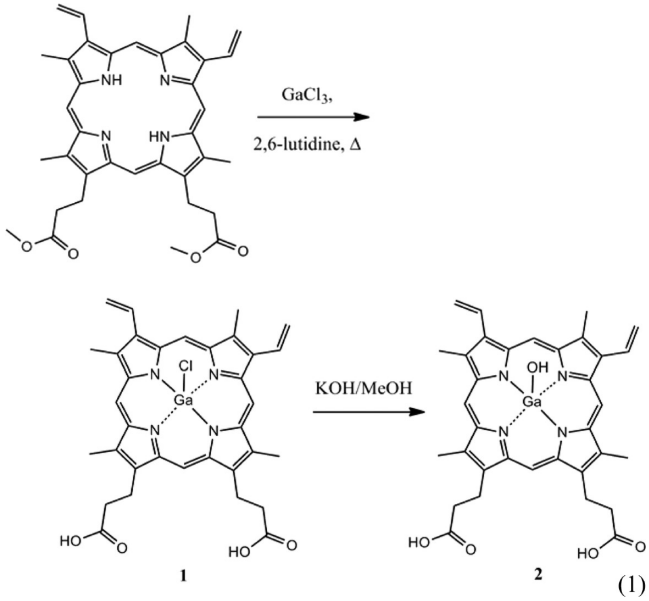

because reactivity with silica and alumina limits purification options. When heated at reflux in 2,6-lutidine rather than pyridine metalation occurs at atmospheric pressure, and when an excess of gallium salt is employed the reaction is driven to completion. Prior reports have used high pressure reactors with pyridine at reflux to effect metalation. We find that the substitution of 2,6-lutidine as the solvent allows for the use of atmospheric pressure with no loss of yield. Filtration following dissolution of the product in methanol affords a purification step to separate any unreacted porphyrin. Under these conditions the methyl ester is saponified and so in a single step Ga(PPIX)Cl (**1**) is produced directly without need of a deprotection step, becoming the diacid upon acidic aqueous workup. Whether the excess gallium salts or the gallium porphyrin complex product is promoting ester hydrolysis is undetermined. Potassium hydroxide was used to substitute chloride for hydroxide. Ga(PPIX)Cl and Ga(PPIX)(OH) (**2**) were isolated as light-sensitive purple-red solids in 80−85%

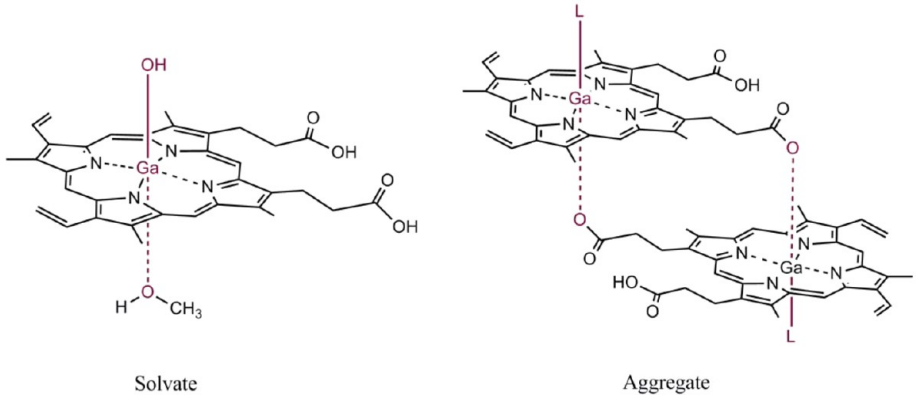

Figure 2. Solution behavior of Ga(PPIX) is mediated by solvation, which is in competition with self-interactions between the propionic acid groups and the "free" site on the metal. In the transient system, identity of the sixth axial ligand is denoted as "L" due to exchange between water, methanol, and hydroxide-ligated species. Full cyclization is proposed to be favored over dimerization through one metal−oxygen bond because of lability at the metal, simple proximity, and the chelate effect.

dx.doi.org/10.1021/ic301106g | *Inorg. Chem.* 2012, 51, 10747−10761

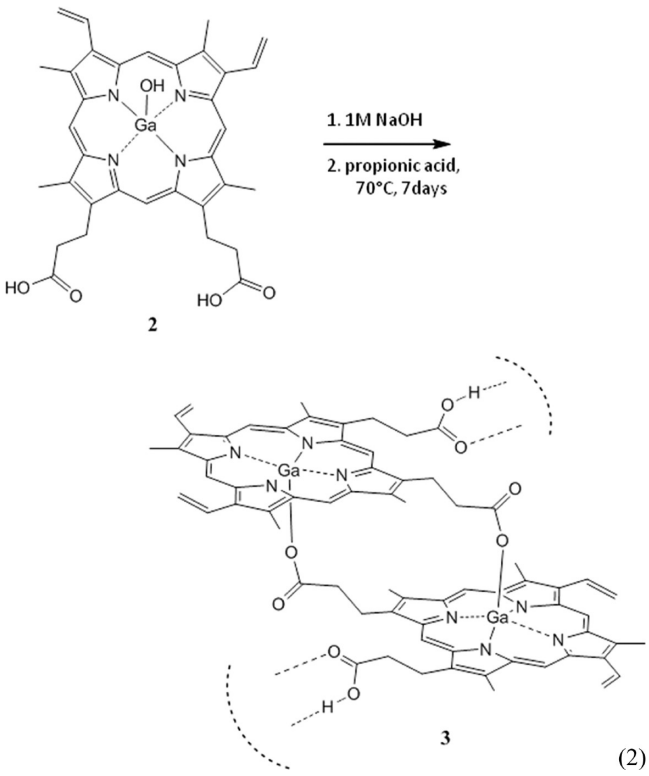

(2)

yields (eq 1). Elemental analysis indicates the final solid product (**2**) is a hydrate but this has been difficult to confirm by DSC or NMR. Differential scanning calorimetry of the isolated solid Ga(PPIX)(OH) exhibited no exothermic or endothermic changes in the range 25−200 °C.

We have adapted the acid-catalyzed synthesis of hematin anhydride[33,34] to the gallium porphyrin to give **3**, an insoluble gallium analogue of hematin anhydride (eq 2) which can be isolated by centrifugation in trace to 5% yields. The propionate-bridged reciprocal dimer $[Ga(PPIX)]_2$ IR spectrum includes the 1713 cm^{-1} and 1665 cm^{-1} ν_{asym} (CO) and 1223 cm^{-1} ν_{sym} (CO) bands indicative of monohapto- carboxylate-metal binding[35,36] (Figure 3). This and the insolubility of the compound combine as strong evidence that we have formed a dimer which is analogous to the natural biocrystalline hemozoin. Attempts to optimize the yields for the formation of **3** beyond trace levels have not been successful to date.

Probing Self- and Solvent Interactions. In solution, the interactions of Ga(PPIX)(OH) with itself (Figure 2) can be roughly followed by observing chemical shift changes over a range of temperatures or concentrations. Variability in the chemical shift by ^{1}H NMR over a range of temperatures (Figure 4) and concentrations (Figure 5) indicate rapid exchange in solution between two or more states which do not resolve at low temperature. Increased broadening is seen for protons near the propionic acid groups of the porphyrin at higher concentration. In the presence of competing ligands, rapid exchange at the labile axial ligand position is seen for both the natural porphyrin Ga(PPIX)(X) (where X is OH- or Cl-) and the synthetic porphyrin Ga(OEP)(Cl).

When compared with the known literature for the aggregation of diamagnetic metal complexes of natural porphyrins,[25] it is readily apparent that the ^{1}H NMR patterns seen in d_4-methanol are of the minimally aggregated form, and extensively aggregated structures with their characteristic large upfield shifts of the methine protons are not seen. Indeed no deviation from Beers' Law is seen in UV behavior up to the highest concentration tested (9.6×10^{-6} M). Therefore the methanol stabilizes the dissolved metalloporphyrin, most likely by labile coordination with the free sixth axial position as proposed in Figure 2.

The concentration-dependent value of the chemical shift of the protons at the porphyrin periphery by ^{1}H NMR in d_4-methanol indicates a self-reaction that alters the chemical environment of the porphyrin, mostly at the methine proton position between the two propionic acid chains, numbered H(20). This result, combined with the observation that the propionic acid group methylene protons, numbered H(2α), H(18α), and H(2β), H(18β) give broad, overlapped signals which increase in half-width at higher concentrations of Ga(PPIX)(X), is enough to implicate the propionic acid groups as key players in the mechanism of the self-association as depicted in Figure 2. No large upfield shifts of the methine protons are seen at high concentrations, thus close association with the ring current of an adjacent porphyrin unit, or "π-stacking", is not implicated in the interaction.

The strong effects caused by the propionic acid groups have led us to duplicate our experiment utilizing the synthetic porphyrin Ga(OEP)(Cl), which has a similar porphyrin substitution pattern and electronic structures to the protoporphyrin IX. To characterize the electronic structure, absorption and MCD spectral data for Ga(OEP)(Cl) were measured and are compared with previous data for Ga(PPIX)(OH)[10] and Zn(OEP).[38] TD-DFT calculations were also carried out and the results compared with Ga(PPIX)-(OH) from our previous work.[10]

The ESI mass spectral data, as with the Ga(PPIX)(OH), show predominantly the monomeric Ga(OEP) at 601.2834 (calculated: 601.2816 amu). The region at 1239.58 amu shows the presence of a number of μ-oxo axially coordinated species of the dimer, Figure 6. Previous ESI studies of Ga(PPIX) showed no evidence of μ-oxo dimer; rather, dimerization through the propionates was supported by the masses observed.[39] Note that from the ESI little if any trimer is present and thus if there is any trimerization it will have only minor effects on the dimerization equilibrium constants calculated here. The gallium octaethylporphyrin μ-oxo dimer is protonated [$(C_{36}H_{44}N_4Ga)_2(OH)$: 1219.567 calculated, 1219.568 observed] and a water molecule [$(C_{36}H_{44}N_4Ga)_2(OH)(H_2O)$: 1237.577 calculated, 1237.580 observed] as well as coordinated to a methoxide and water [$(C_{36}H_{44}N_4Ga)_2(OMe)(H_2O)$: 1251.593 calculated, 1251.587 observed] and finally to a methoxide and methanol [$(C_{36}H_{44}N_4Ga)_2(OMe)(HOMe)$: 1265.608 calculated, 1265.608 observed]. The formation and observation of dimers in the mass spectrum is dependent on the μ-oxo dimerization.

The absorption and MCD spectra, Figure 7, are typical of low spin transition metals or main group M(OEP) complexes. The MCD spectrum shows a Q_{00} band centered on 568 nm with the vibrational bands near 531 nm. For Zn(OEP), we find Q_{00} at 564 nm followed to the blue by a series of vibronic bands, Q_{vib}. The B band is centered in the Ga(OEP) on 398 nm exhibiting a very intense and well-resolved, positive A term indicating the nondegenerate nature of the ground state and the unsplit nature of the degenerate S_2 excited state. The high symmetry of the HOMO, HOMO-1, LUMO and LUMO+1 is typical of OEP, reflecting the symmetric nature of the peripheral substituents. The MCD spectrum of the Zn(OEP)[38] also shows an intense and well-resolved A term centered on 401 nm. The slight blue shift in the B band from 401 nm of the Zn(II)(OEP) to the 398 nm of the Ga(III)(OEP) most likely arises from the electron withdrawing effects of the 3+ oxidation state of the gallium. Finally, the shoulder that is seen at a

dx.doi.org/10.1021/ic301106g | Inorg. Chem. 2012, 51, 10747−10761

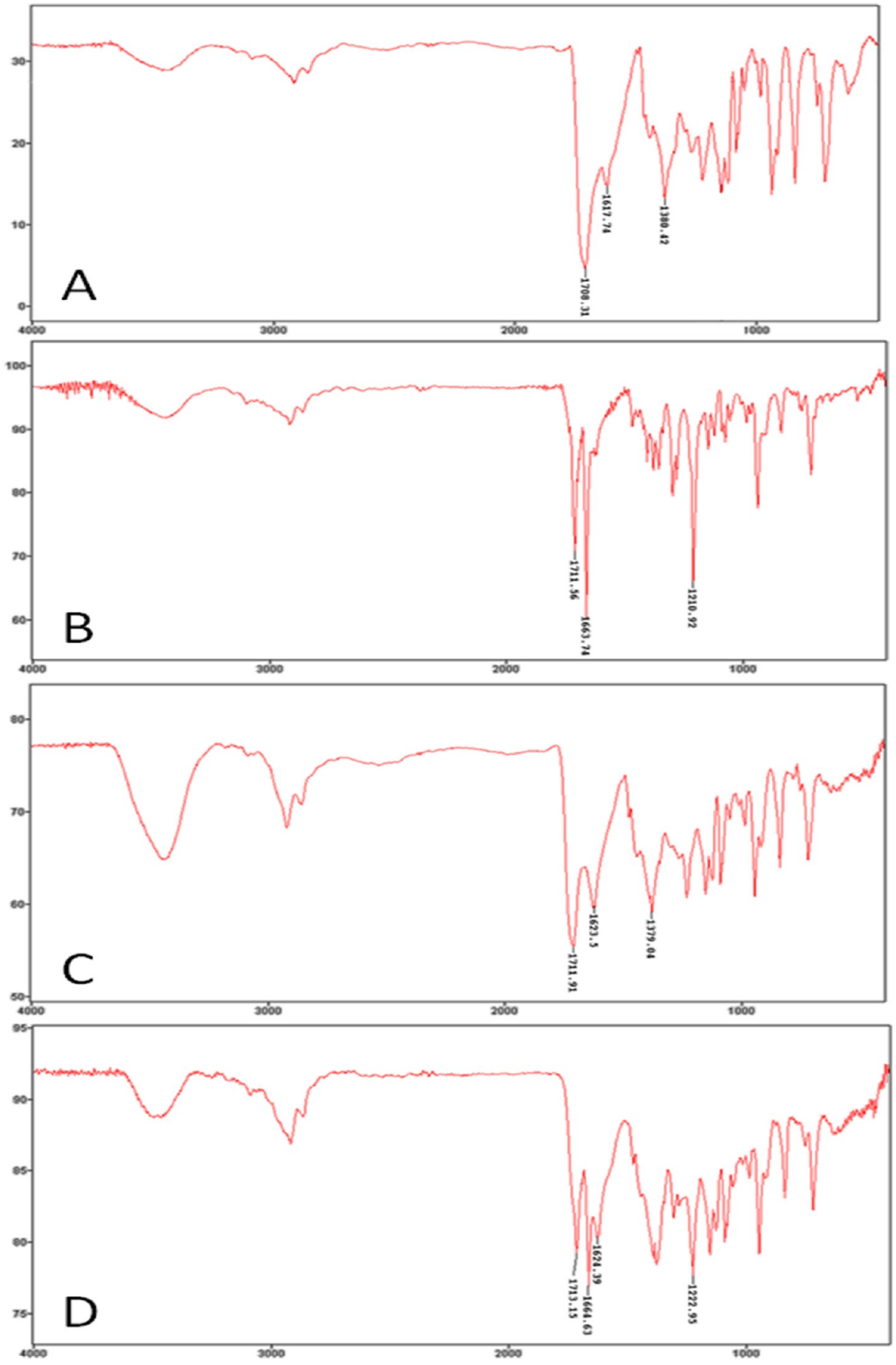

Figure 3. IR spectra of monomeric and dimeric M(III)(PPIX) species for comparison purposes: (A) free acid hematin Fe(III)(PPIX)(OH), denoted peaks: (cm^{-1}, ± 1 cm^{-1}) 1708, 1618, 1380; (B) hematin anhydride synthetic dimer, denoted peaks: (cm^{-1}, ± 1 cm^{-1}) 1712, 1664, 1211;[37] (C) gallium(III) protoporphyrin IX hydroxide, denoted peaks: (cm^{-1}, ± 1 cm^{-1}) 1712, 1624, 1379; (D) dimeric gallium(III) protoporphyrin IX with monomer impurity, denoted peaks: (cm^{-1}, ± 1 cm^{-1}) 1713, 1665, 1624, 1223.

dx.doi.org/10.1021/ic301106g | *Inorg. Chem.* 2012, 51, 10747−10761

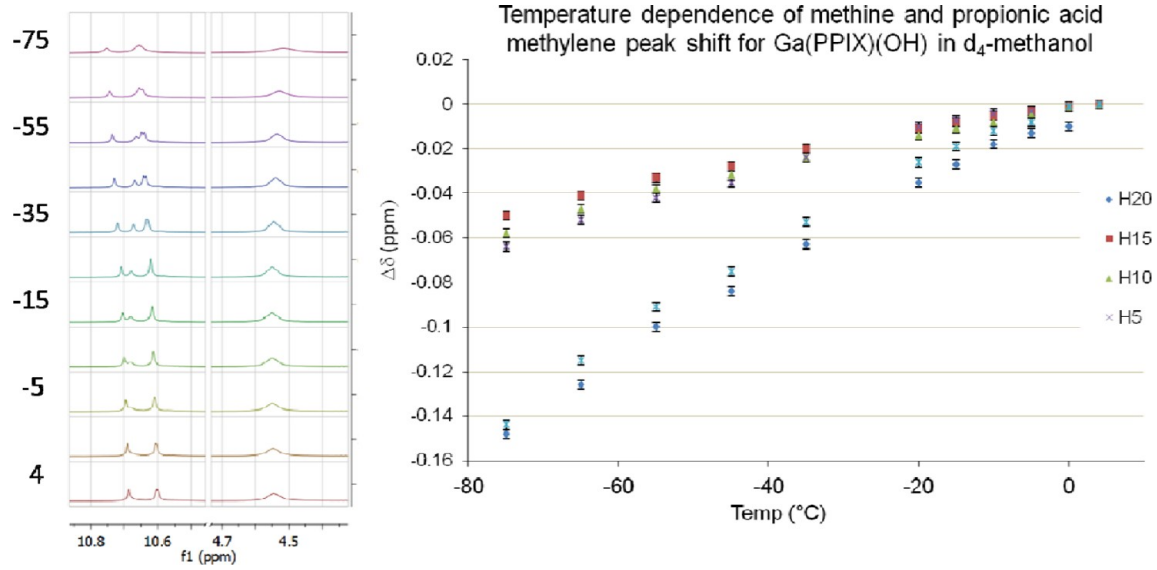

Figure 4. Selected peak shifts for variable-temperature NMR of Ga(PPIX)(OH) showing clear upfield shift of the methine proton between the two propionic acid side chains and the acid chain methylene protons at lower temperatures.

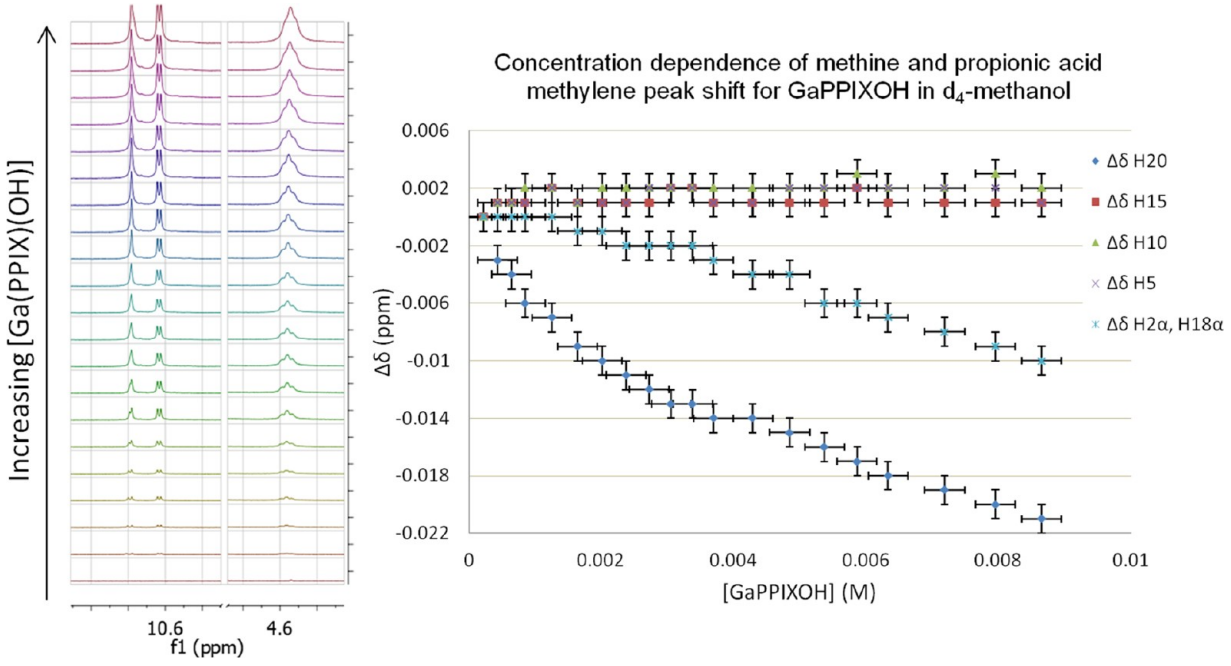

Figure 5. Selected peak shifts for concentration dependence experiment showing upfield shift of the methine proton between the two propionic acid side chains and the acid chain methylene protons at increased concentrations.

slightly lower energy to the B-band near 410 nm would suggest the presence of a species with probably a second ligand coordinated to the Ga(OEP). While the ESI mass spectral data did not show any axial ligand coordination for the monomeric Ga(OEP) species, the dimer clearly showed multiple axial ligation states.

Ga(OEP)Cl exchanges ligand Cl^- slowly over time with methanol upon dissolution of the solid to yield the methoxy adduct, as determined unambiguously by X-ray crystallography of the solid which crystallizes upon concentration.[40] No change in chemical environment is determined by either NMR or UV analysis of Ga(OEP)X in methanol solution; thus, we conclude that the exchange dynamics lead to an average spectrum that does not change appreciably. Crystals of Ga(OEP)(OMe) grow spontaneously in solutions of Ga(OEP)X in methanol, and form much faster from Ga(OEP)(OH) or Ga(OEP)Cl in presence of any strong base.[40] In short, the ligand exchange is rapid and favors the "hardest", most electronegative anionic ligand. The porphyrin stacking and side chain orientation have been found to be comparable to those in known gallium porphyrin structures.[18,41,42] No change in chemical environment is determined by either NMR or UV analysis of Ga(OEP)(X) in methanol solution; thus, we conclude that the exchange dynamics leads to an average spectrum that does not change appreciably.

Of particular importance to the study of metalloprotoporphyrin IX self-interaction and dimerization, the binding constant of acetate is orders of magnitude larger for Ga(OEP) species than for Ga(PPIX) species. This indicates competition

dx.doi.org/10.1021/ic301106g | Inorg. Chem. 2012, 51, 10747−10761

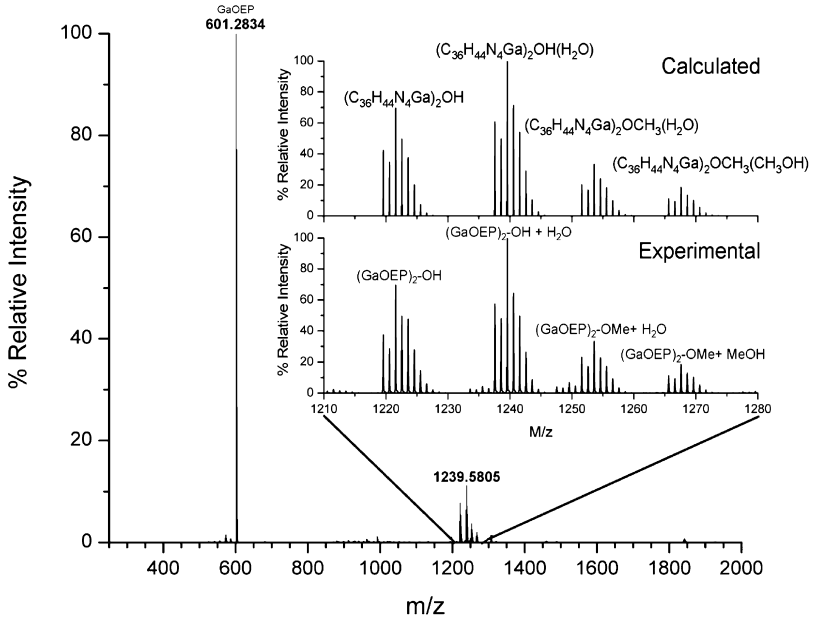

Figure 6. ESI mass spectral data of Ga(OEP) species in 100% MeOH. The speciation in the dimer region is indicated in the expanded inset. The calculated mass isotope patterns are shown above the experimental data with the identified speciation.

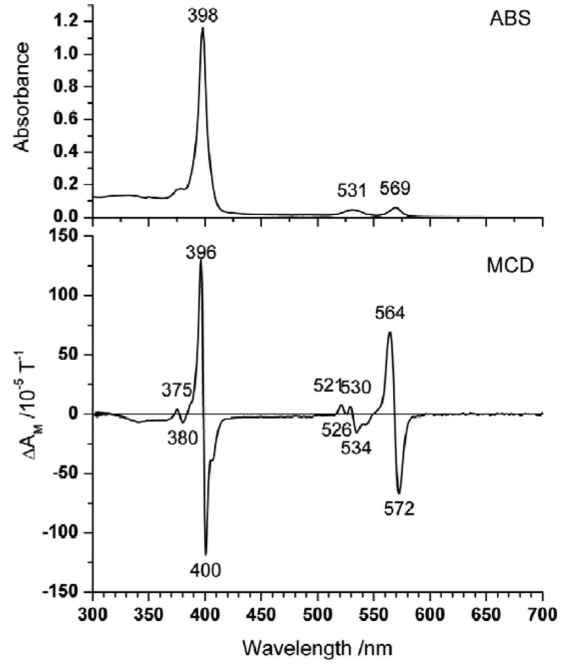

Figure 7. UV−visible absorption and MCD spectra of GaOEP dissolved in 100% MeOH. The absorption at 531 nm is actually composed of multiple overlaying transitions as shown by the convoluted MCD below. The shoulders present (especially toward the red) of the B-band and the complexity of the Q-band region may indicate multiple solution speciation.

from the porphyrin's own acidic side-chains in the case of protoporphyrin IX species. In an effort to establish that the self-interaction of Ga(PPIX)(X) derives from an interaction between the metal center and the propionic acid side chains, we have undertaken as series of tests against acetic acid, utilizing both Ga(PPIX)X and Ga(OEP)Cl. The corresponding reaction involving Ga(OEP)(OH) could not be performed because of rapid precipitation of crystals of the methoxide adduct, Ga(OEP)(OMe), before titrant could be added. Such crystals also form rapidly upon addition of any base to solution of Ga(OEP)Cl in methanol. Addition of one equivalent of acetic acid immediately following dissolution prevents this rapid reaction with the solvent and consequent precipitation, giving a stable pink solution in methanol, and causes crystals of Ga(OEP)(OMe), once formed, to redissolve. We compared these results with the concentration-dependent shifts of the protoporphyrin IX species discussed previously, confirming that a dehydration reaction resulting in ligation of acetate which competes with propionic acid groups of the porphyrin for coordination at the gallium. The results of the titrations are summarized in Table 1.

The reaction of Ga(PPIX)(X) with itself is analogous to that of Ga(OEP)Cl with acetate (eq 3). Use of acetic acid rather than acetate mimics the propionic acid groups of the protoporphyrin IX and avoids deprotonation of these groups.

Given the strength of the binding of acetate to Ga(OEP)Cl compared to the value of near unity for that of acetate to Ga(PPIX)(X), the conclusion we make is that this loss of affinity for acetate is due to competition with the binding of the propionate side chains in the case of Ga(PPIX)(X). Both are in dynamic equilibrium, and therefore we end up with the equilibria shown in eq 4.

The immediate implication is that interactions between the propionic acid side chains and the metal are much stronger than porphyrin-porphyrin π-interactions. This equilibrium is a dynamic, rapid-exchange process which leads to oligomeric species in solution. These would be short-lived because of the lability of the axial position in methanol solution, though the chelate effect will favor the reciprocal dimer.

It becomes relevant to compare these interactions with simple deprotonation. Titration of Ga(PPIX)(X) against strong base, Figure 8, yields a characteristic spectrum in which the side of the porphyrin experiencing the largest upfield shift is actually the side with vinyl substituents. As a first equivalent of base is added, propionic acid group methylene protons exhibit increased broadening to indicate a slowing of overall equilibrium exchange rate, and as the amount of base present increases

dx.doi.org/10.1021/ic301106g | Inorg. Chem. 2012, 51, 10747−10761

Table 1. Association Constants from WinEQNMR2

	K_{eq} (no units)
$2Ga(PPIX)(OH) \rightleftharpoons [Ga(PPIX)]_2 + nH_2O$	1.26 ± 0.10
$2Ga(PPIX)(Cl) \rightleftharpoons [Ga(PPIX)]_2 + n$HCl	1.93 ± 0.13
$Ga(PPIX)(OH) + AcOH \rightleftharpoons Ga(PPIX)(OAc) + H_2O$	6.9 ± 0.03
$Ga(PPIX)(Cl) + AcOH \rightleftharpoons Ga(PPIX)(OAc) + HCl$	0.2 ± 0.03
$Ga(OEP)(Cl) + AcOH \rightleftharpoons Ga(OEP)(OAc) + HCl$	$(2.694 \pm 0.17) \times 10^{+3}$[a]

[a]No shift in ^{1}H NMR chemical shift was observed for Ga(OEP)Cl in d_4-methanol over a concentration range of 0.03 to 0.0003M

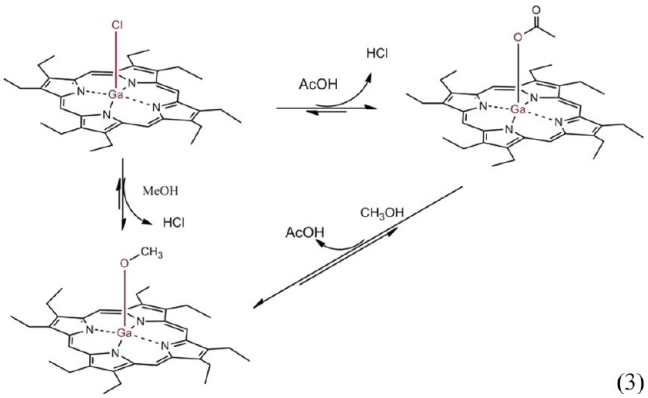

(3)

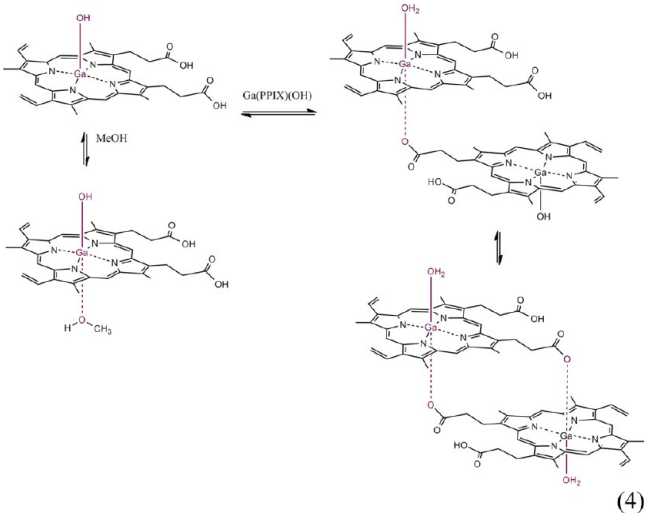

(4)

these signals sharpen into distinct triplets not seen in neutral or acidic solution. On the basis of this, we can regard the simple deprotonation of both acid groups as having a very different NMR signature than that seen upon dilution or in ligand exchange chemistry.

The reaction of Ga(PPIX)(X) (where X = OH or Cl) with fluoride ion is of particular interest as the reaction exchange is slow on the NMR time scale. The Ga−F bond is known to be particularly strong;[43] however, it is seen to be labile in the case of gallium porphyrin fluoride species, and a dynamic equilibrium is established in methanol solution as in all other cases. On addition of fluoride source (CsF or NBu_4F) to gallium(III) protoporphyrin IX, we see the establishment of a slow equilibrium in which a third compound exists in slow exchange with the starting material and main product. This decreases in concentration on addition of more fluoride to give a main product which is Ga(PPIX)F with an IR ν_{Ga-F} band at 499 cm^{-1} in solid state. The identity of the counterion in the fluoride salt was found to have no effect, although fluoride sources with nonreactive cations were chosen.

In the ^{1}H NMR spectrum, this third compound is distinguished by a large methine peak shift to a more upfield region of the spectrum, and splitting of all porphyrin proton signals into two separate sets of signals of equal intensity in a manner that indicates two chemically unequal but bound porphyrin units in the molecule. Analogous patterns of upfield shift and splitting of porphyrin signals is seen in the ^{1}H NMR spectra of the μ-hydroxy bridged dimer of Ga(OEP),[39] which was determined by X-ray crystallography to have a single water molecule bound to one of the gallium atoms and to have staggered conformation in the position of the ethyl groups around the porphyrin periphery, and by Ponomarev et al.[44] whose studies compared octaethylporphyrin bound by either a cis- or a trans- ethene bridge. The methine shift to an upfield region of the spectrum indicates that the methine of one porphyrin is located in range of the aromatic ring current of the second in the third compound observed by NMR, Figures 9, 10, and 11. For these reasons we tentatively assign the third compound as a dimeric μ-fluoro bridged species similar to that seen by Guillard et al.[20] There is an interesting contrast in the μ-fluoro and the μ-oxo gallium(III) dimers where the μ-fluoro is readily observed even at low concentrations of fluoride, while the μ-oxo dimer requires very high concentrations of base for the Ga(III)(PPIX) to be observed in solution For the related Fe(III)porphyrin complexes the μ-oxo bridged species are remarkably stable. This phenomenological distinction is due to the strong antiferromagnetic coupling of the two Fe(III) centers in $[Fe(III)(porphyrin)]_2O$, and this coupling is of course not available for $S = 0$ Ga(III) with its d^{10} configuration. On the other hand, Ga(III) porphyrins, like high spin Fe(III) porphyrins, are excellent Lewis acids and for the gallium species this translates as a high fluorophilicity.

Support for this assignment is found in the ^{19}F NMR spectra, Figure 10C, where the free F^- salt appears as a singlet at −153.6 ppm. Ga(PPIX)F gives a singlet at −159.1 ppm matching that of a corresponding known polymeric compound Ga(OEP)F,[19] and the third compound gives a pair of peaks at −156.2 ppm and −156.4 ppm of roughly equal intensity which must correspond to a near equal population of both diastereomers of porphyrin dimer.

In the case of Ga(PPIX)(OH), following substitution of HO^- with F^- at the gallium, Ga(PPIX)F reacts with further Ga(PPIX)(OH) in solution to give the μ-fluoro bridged dimer. We assume facile deprotonation of acid groups by free hydroxide in the case of Ga(PPIX)(OH). Equilibrium constants were determined graphically using simple linear regression (Table 2).

Similar μ-fluoro bridged gallium porphyrin species are known in the literature;[20,45] however, the solution behavior of these compounds has not been explored, and this is to our knowledge the first report of ^{1}H and ^{19}F NMR of such a species in solution. That this species exists in a reaction that ultimately yields a simple substitution of an anionic ligand on the gallium is unexpected, and can be partially explained by the very high affinity of Ga(III) metal for fluoride.

The slow rate of exchange is dependent on the presence of carboxylic acid groups, and it is not seen in the corresponding reaction with Ga(OEP)(X), which gives an averaged signal corresponding to a fast equilibrium, Figure 11. Repeating the Ga(OEP)(X) titration against CsF with 2 equivalents of acetic acid present slows the rate of exchange via competitive

dx.doi.org/10.1021/ic301106g | Inorg. Chem. 2012, 51, 10747−10761

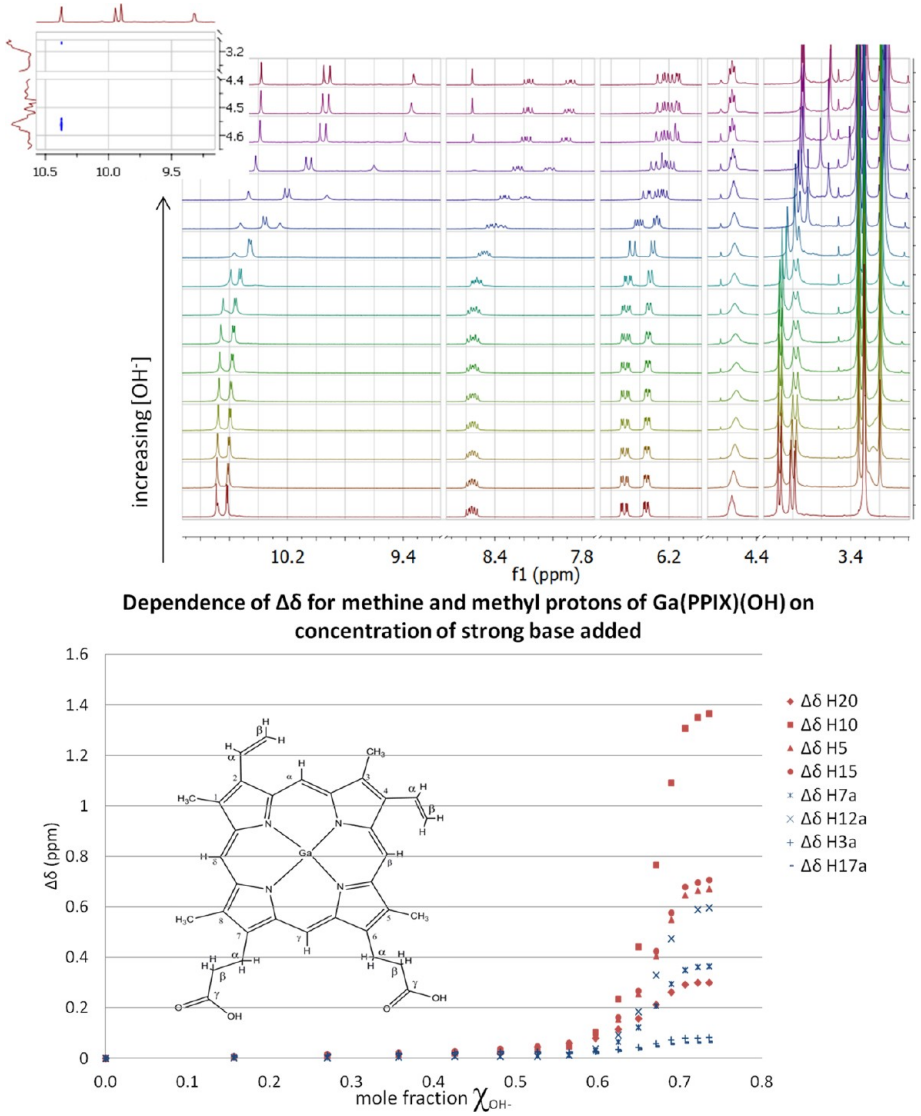

Figure 8. Top: stacked spectra of titration of Ga(PPIX)(OH) against NMe_4OH in d_4-methanol; inset: NOESY of methine region confirms the most downfield methine proton is located between the propionate groups. Bottom: plot of peak shift vs mole fraction of strong base added demonstrates sharp change upon addition of second equivalent of base.

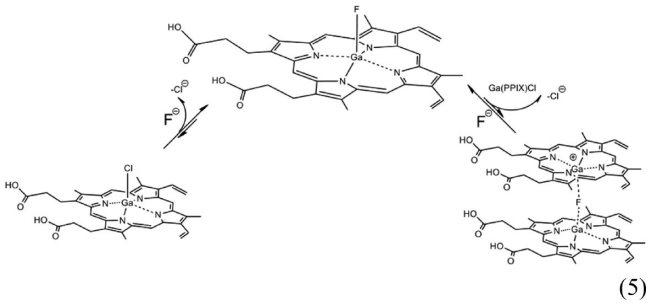

(5)

inhibition to the point that the signals of reagent and product are no longer averaged and emerge as two separate sets of signals. However, the μ-fluoro bridged gallium porphyrin species is not seen in solution in this instance, leading to the conclusion that the propionic acid groups are responsible for inhibiting the substitution at the gallium binding site but the presence of molecules with carboxylic acid groups in solution is not enough to form a μ-fluoro bridged porphyrin dimer in solution. The Ga(PPIX) μ-fluoro bridged dimer is likely to be stabilized by intermolecular propionic acid interactions between the bridged porphyrins.

The splitting patterns observed in the ^{1}H NMR of the dimer are indicative of a high degree of rigidity in the propionic acid groups, Figure 13. The bridged structure supported by the literature and the methods outlined above cannot account for propionic acid group rigidity on its own. Nor can isomerism in the porphyrin orientation, as this would not cause the specific differences seen and is not supported by peak integration ratios in the dimeric species which correspond to a racemate in the dynamic system observed. In the absence of added intermolecular forces the Ga−F bonds would be free to rotate, as would the C−C bonds of the side chain groups. What we see, however, is the formation of a rigid conformation.

We know, based on simple analysis of ^{1}H NMR spectra, that the new species must be composed of two chemically inequivalent porphyrin units overall, which are always present in equal ratio. This could indicate two inequivalent porphyrins which are bound directly, or isomerism in the porphyrin pairs formed, with some porphyrins "flipped" to give the other

dx.doi.org/10.1021/ic301106g | Inorg. Chem. 2012, 51, 10747−10761

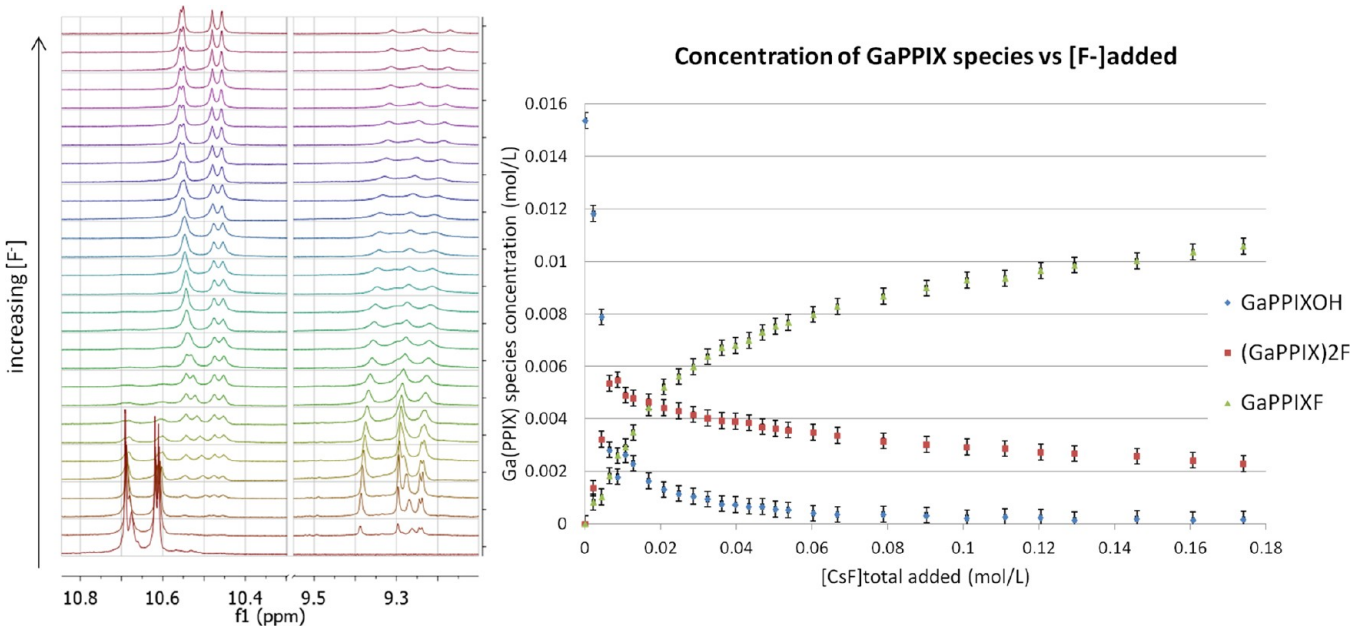

Figure 9. Stacked plots of methine region of ^{1}H spectra (initial spectrum at the bottom, top spectrum is final addition) used to plot the concentrations of each species over the course of titration shown in the graph at the right. Ga(PPIX)(OH) methine protons in range 10.60−10.71 ppm; $[Ga(PPIX)]_2F$ methine protons in range 9.15−9.40 ppm; Ga(PPIX)F methine protons in the range 10.45−10.58 ppm. [GaPPIX] species values in the graph were corrected for a slight dilution.

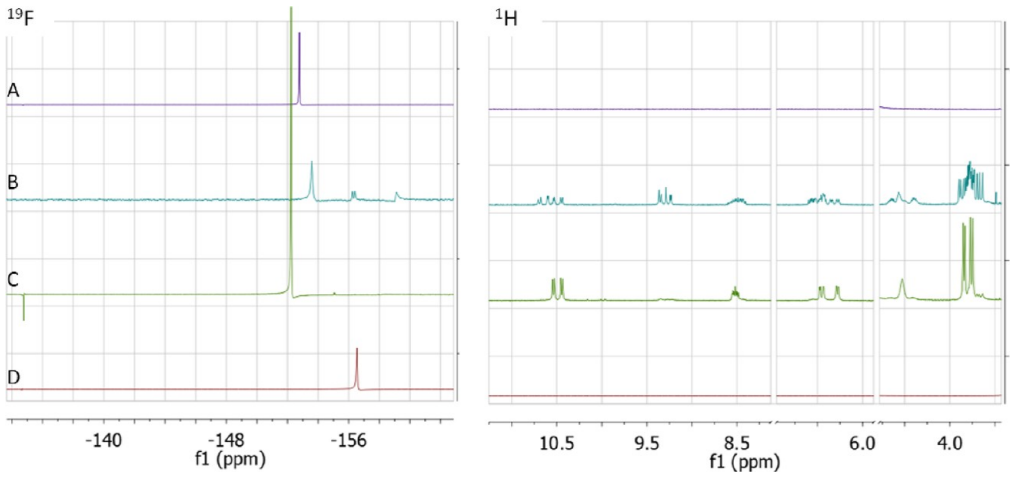

Figure 10. Stacked for comparison: (A) NBu_4F alone; (B) 1:1 molar ratio Ga(PPIX)(X) (with component ratios as follows, 1 Ga(PPIX)(OH): 0.96 Ga(PPIX)F: 0.72 $(Ga(PPIX))_2F$): NBu_4F; (C) 1:25 molar ratio Ga(PPIX)F: NBu_4F (Ga(PPIX)F broad, ^{19}F = −159.1 ppm); (D) 1:2 molar ratio propionic acid: NBu_4F. left ^{19}F NMR; right ^{1}H NMR. Internal standard, NBu_4F peaks and areas without signals in ^{1}H spectrum were omitted for clarity.

diastereomer. Both diastereomers would be in slow exchange with monomer and starting material. As well, close inspection of the splitting in the propionic acid group α-methylene peaks tells us that we have two sets of chemically inequivalent protons with overlapping signals, each split by three unequal protons leading to the octets observed.

The splitting pattern observed appears to arise from self-interaction at the propionic acid groups which would be accompanied by lack of rotation about the Ga−F−Ga. This would hold the structure in the semirigid conformation required by the experimental evidence. Possible structures of this type which would agree with the splitting observed are described in Figure 14; possibilities involving interaction of propionic acid groups of the same porphyrin unit are discounted, as such structures have not been observed in known monomeric protoporphyrin IX species. Such a structure would also be too geometrically strained to be considered as a candidate. It is expected that the rate of dynamic exchange between any orientations of hydrogen bonding would actually be fast on the NMR time scale; thus, we have both fast-exchange and slow-exchange processes occurring at once. The average position of each α-methylene proton, therefore, is what is seen. The proton peak assignment is detailed in Figure 12B.

We are keen to understand the electronic role of the peripheral side chains in moderating the iron-based chemistries of heme proteins. The comparison of Ga(III) octaethylporphyrin and protoporphyrin IX species provides an opportunity to compare both the optical data and the electronic structure in the presence and absence of the propionic acid side chains. Figure 15 shows the energies and isosurfaces of the six highest

dx.doi.org/10.1021/ic301106g | Inorg. Chem. 2012, 51, 10747−10761

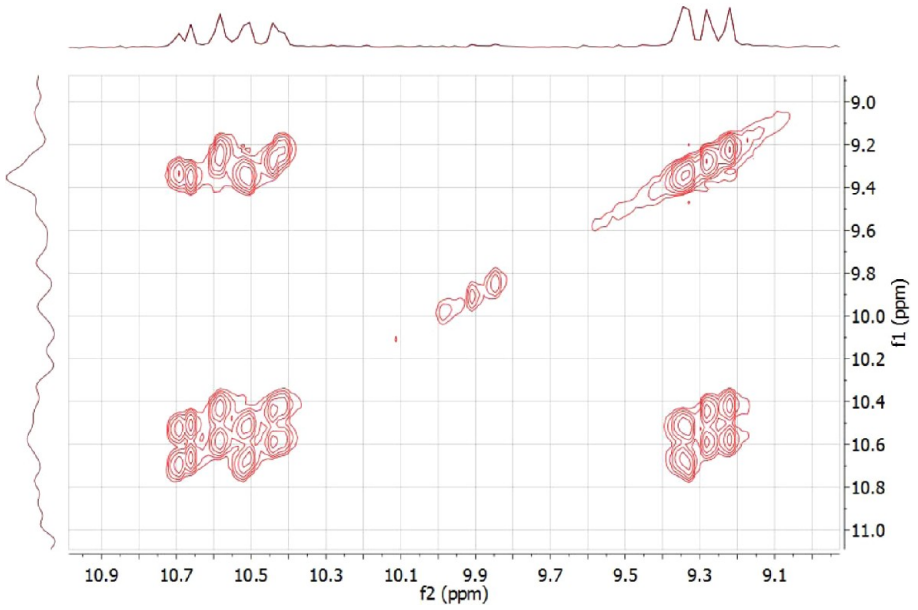

Figure 11. 2D exchange peaks (negative) in NOESY NMR spectrum indicating exchange between the 3 sets of methine protons in solution.

Table 2. Association Constants for Fluoride Coordination

	apparent K_{eq} [a]
$Ga(PPIX)(OH) + CsF \overset{K_1}{\rightleftharpoons} Ga(PPIX)F + CsOH \overset{K_2}{\rightleftharpoons} [Ga(PPIX)F]^-Cs^+ + H_2O$	3.41 ± 0.01
$Ga(PPIX)F + Ga(PPIX)OH \overset{K_3}{\rightleftharpoons} [Ga(PPIX)]_2F^+OH^-$	$(1.1 \pm 0.1) \times 10^3$
$Ga(PPIX)Cl + CsF \overset{K_1}{\rightleftharpoons} Ga(PPIX)F + CsCl$	4.16 ± 0.01
$Ga(PPIX)F + Ga(PPIX)Cl \overset{K_3}{\rightleftharpoons} [Ga(PPIX)]_2F^+Cl^-$	$(9.6 \pm 0.6) \times 10^2$

[a]Apparent K_{eq} refers to K_n as described above. The complexity of the system made it necessary to ignore the effects of proton transfer in the determination. This assumption leads to a higher degree of error in the dimer formation equilibrium constant than would be seen in a simple system. Deviation from linearity in the graphical determination at higher concentrations suggests that there is cooperativity in the formation of the dimer.

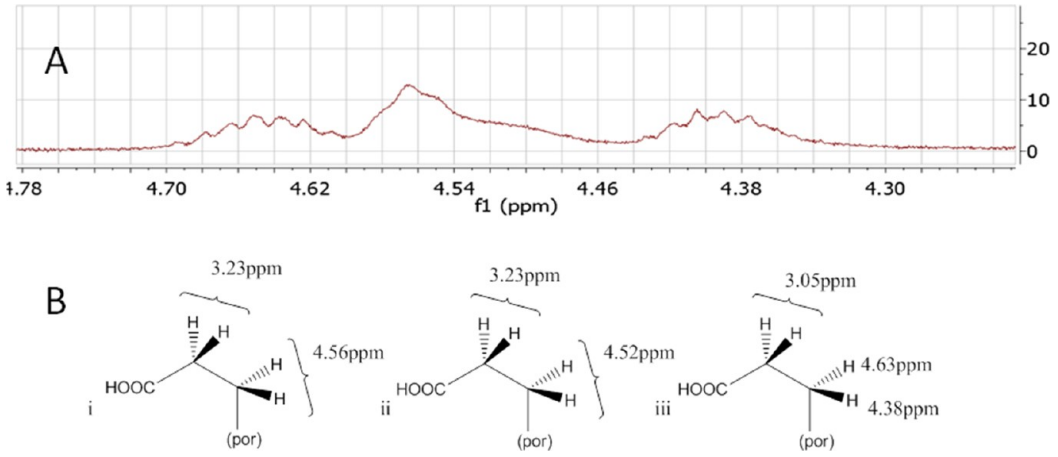

Figure 12. (A) Close-up of propionate α methylene ^{1}H NMR peaks of all three compounds. Note that the intermediate splits into an apparent doublet of octets which is actually two overlapped sets of doublets of doublets of doublets at 4.53 ppm and 4.47 ppm, respectively; (B) assignment of peaks: (i) Ga(PPIX)F, (ii) Ga(PPIX)(OH), (iii) $[Ga(PPIX)]_2F$; in all species the protons of the chemically inequivalent propionate groups are very similar in shift.

occupied and unoccupied molecular orbitals (MOs) for both Ga(OEP) and Ga(PPIX) species. The transition data, Table 3, lists the combinations of one-electron transitions that make up the optical transitions to the Q-band comprising an overlap of

dx.doi.org/10.1021/ic301106g | Inorg. Chem. 2012, 51, 10747−10761

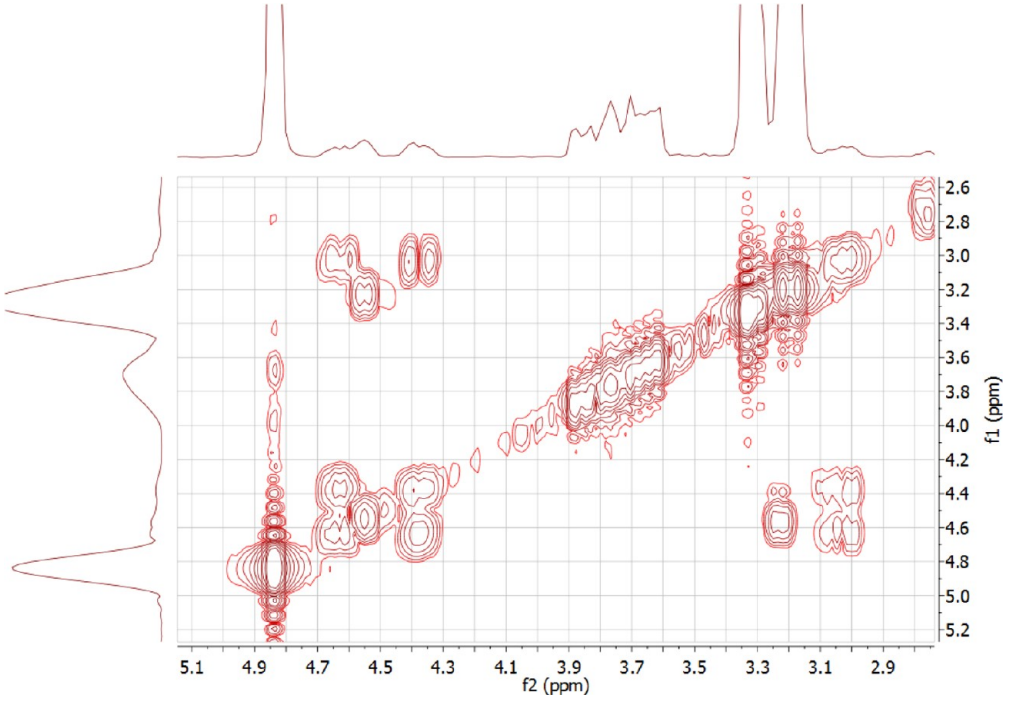

Figure 13. COSY NMR 2D spectrum of mixture Ga(PPIX)(OH)/μ-fluoro-bridged dimer/Ga(PPIX)F. Focus on methylene region clearly exhibits separation of 4 distinct α methylene signals, two of which arise from the presence of bridged species.

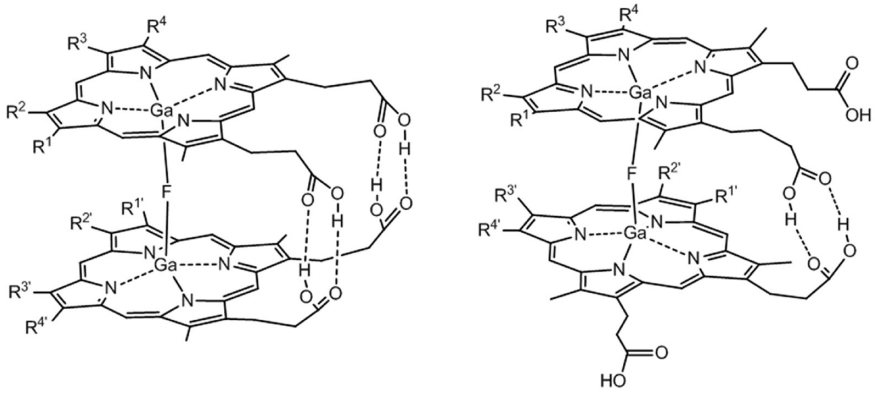

diastereomer a:	$R^1=R^{1'}=R^3=R^{3'}$	methyl
	$R^2=R^{2'}=R^4=R^{4'}$	vinyl
diastereomer b:	$R^1=R^{4'}=R^3=R^{2'}$	methyl
	$R^2=R^{3'}=R^4=R^{1'}$	vinyl

Figure 14. Proposed orientation of hydrogen bonding within a μ-fluoro-bridged dimer of Ga(PPIX) based on NMR coupling evidence. All would coexist in a dynamic exchanging system.

State 2 and State 3 to form the near degenerate excited state. The very small energy difference between the top two filled MOs, often referred to as Δ ($HOMO_{0-1}$, for both complexes is relatively small, with Ga(OEP) = 0.163 eV and Ga(PPIX) = 0.1088 eV. These low values are reflected in the very weak Q-band oscillator strength for Ga(OEP) and Ga(PPIX), neither of which are as low as those calculated for Zn(PPIX) or Zn(TPP) (where TPP refers to 5,10,15,20-tetraphenylporphyrin).

MO calculations of porphyrins provide three important facets of the electronic structure: (i) the splitting energies (ΔE) between the top two filled and bottom two unoccupied MOs, (ii) the HOMO−LUMO gap, and (iii) the electronic distribution around the ring and possibly on to the peripheral atoms, especially at the HOMO and LUMO energy levels. In previous reports,[38] we have shown that the trend in "$\Delta HOMO_{(0-1)}$" correlates strongly with both the oscillator strength of the Q-band and the Q-B energy gap, $E_{B\text{-}Q}$. The Q bands at 569 nm (Ga(OEP)) and 578 nm (Ga(PPIX)) exhibit almost identical absorbance, meaning the same oscillator strengths. This fits the trends reported previously.[10] Although the calculated oscillator strengths of the sum of the two transitions (0.031 and 0.025 for Ga(PPIX) and Ga(OEP), respectively) reverse the trend in which increases in $\Delta HOMO_{0-1}$ increase the oscillator strength, this is perhaps because of the overlap of MOs 153 and 152 compared with the clear separation of 157 (HOMO-1) from 156 (HOMO-2) for

dx.doi.org/10.1021/ic301106g | Inorg. Chem. 2012, 51, 10747−10761

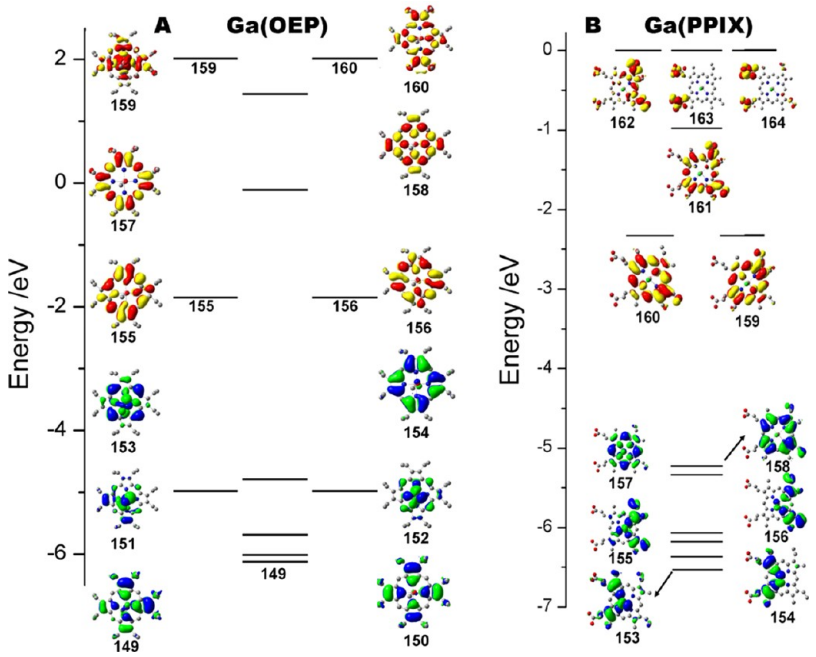

Figure 15. Calculated molecular orbital (MO) energy level diagram for (A) Ga(OEP) from HOMO-5 (MO 149) to LUMO+5 (MO160); E[HOMO-(HOMO-1)] = 0.163 eV and E[(LUMO+1)-LUMO] = 0.27 eV, and (B) Ga(PPIX) from HOMO-5 (MO 153) to LUMO+5 (MO164); E[HOMO-(HOMO-1)] = 0.1088 eV and E[(LUMO+1)-LUMO] = 0.27 eV. The molecular orbital surfaces are also shown at the 0.02 isosurface value level. The phases of the occupied MOs are colored blue and green while the unoccupied MOs are colored red and yellow.

Table 3. Summary of the Q-Band Calculated One-Electron Contributions to the Excited State Transitions of Ga(PPIX) and Ga(OEP) from TD-DFT Calculations[a]

State 1		State 2	
535.06 nm	f = 0.0168	534.12 nm	f = 0.0140
Ga(PPIX)			
157 → 159	0.1151	157 → 159	−0.4748
157 → 160	0.4695	157 → 160	0.1175
158 → 159	0.5142	158 → 159	0.1200
158 → 160	−0.1235	158 → 160	0.5087
State 1		State 2	
524.55 nm	f = 0.0147	523.39 nm	f = 0.0105
Ga(OEP)			
152 → 155	−0.1649	152 → 155	0.1319
152 → 156	−0.1249	153 → 155	−0.4647
153 → 155	−0.1964	153 → 156	−0.1378
153 → 156	0.4153	154 → 155	−0.1218
154 → 155	0.4979	154 → 156	0.4981

[a]The calculated energy (in nm) and oscillator strength (f) are provided.

the Ga(PPIX). The HOMO−LUMO gap also is valuable in predicting the $E_{B\text{-}Q}$ and this was shown in Pinter et al.[10] to quite closely follow the trends of the other porphyrins.

Finally, the MO surfaces provide a graphical image of the distribution of electronic charge for each of the MOs. This allows for an estimation of the effects particularly of peripheral substitution on the visible region optical spectrum, which is governed by the properties of the top 3 or 4 occupied and the lowest 2 unoccupied MOs. The HOMO for the symmetric Ga(OEP) (154) is a typical a_{1u} MO with the 4 nodes aligned through the pyrrole nitrogens, the methane bridges, and the central metal. The presence of the methoxide axial ligand is signaled by the appearance of occupied orbitals from that group in 153, 152, and 151. The nodal pattern in 153 identifies it as the a_{2u} partner to 154, and we have used its energy for the $\Delta HOMO_{0-1}$ values. For the Ga(PPIX) we find the pair of HOMO orbitals at 157 and 158, with the nominally a_{1u} also the HOMO. The effect of peripheral substituents is seen in the 155/156 and 153/154 pairs. The unoccupied MOs, 155 upward, are typical of symmetric porphyrins. The corresponding Ga(PPIX) MOs include delocalization on to the vinyl substituents.

CONCLUSIONS

To conclude, we have synthesized and characterized some gallium(III) complexes of natural and synthetic porphyrins and used dynamic NMR to characterize their interactions in solution with exchanging ligands and with themselves. These interactions are all consistent with a system that is in monomer/dimer exchange in solution via bridging propionates, which is kept in solution by the dynamic nature of that interaction in the presence of a stabilizing solvate interaction with methanol. We have observed direct evidence of inter- as well as intra- molecular interaction between porphyrinic propionic acid groups, both between neighboring carboxylic acids and between carboxylic acids and metal. Knowing these effects exist will allow for us to account for them as we use the model compound in solution to explore these interactions in the formation of more biologically relevant complexes with ligands and drugs.

This understanding of the effects of solvation and self-interaction in the gallium(III) model hints at implications for the behavior of free heme in solution in the absence of strong base which induces formation of μ-oxo dimer species, and also highlights the differences that must be kept in mind when comparing the model to heme itself.

dx.doi.org/10.1021/ic301106g | Inorg. Chem. 2012, 51, 10747−10761

AUTHOR INFORMATION

Corresponding Author

*E-mail: Scott.Bohle@mcgill.ca.

Notes

The authors declare no competing financial interest.

ACKNOWLEDGMENTS

This work was supported with funding through CRC, NSERC (M.J.S. and D.S.B.) and the FQRNT (D.S.B.) of Canada as well as through an OGS award to T.B.J.P. We thank Doug Hairsine for ESI-MS technical support and Dr. Viktor Staroverov for assistance with the TD-DFT calculations.

REFERENCES

(1) Worl Health Organization; *World Malaria Report 2010*; WHO Press: Geneva, Switzerland, 2010.
(2) Enserink, M. *Science* **2010**, *328*, 846.
(3) Sullivan, D. J., Jr.; Gluzman, I. Y.; Russell, D. G.; Goldberg, D. E. *Proc. Natl. Acad. Sci. U. S. A.* **1996**, *93*, 11865.
(4) Egan, T. J.; Ross, D. C.; Adams, P. A. *FEBS Lett.* **1994**, *352*, 54.
(5) Pisciotta, J. M.; Coppens, I.; Tripathi, A., K.; Scholl, P. F.; Shuman, J.; Bajad, S.; Shulaev, V.; Sullivan, D. J., Jr. *Biochem. J.* **2007**, *402*, 97.
(6) Egan, T. J. *J. Inorg. Biochem.* **2008**, *102*, 1288.
(7) Hoang, A. N.; Ncokazi, K. K.; de Villiers, K. A.; Wright, D. W.; Egan, T. J. *Dalton Trans.* **2010**, *39*, 1235.
(8) Pagola, S.; Stephens, P. W.; Bohle, D. S.; Kosar, A. D.; Madsen, S. K. *Nature* **2000**, *404*, 307.
(9) Bohle, D. S.; Kosar, A. D.; Madsen, S. K. *Biochem. Biophys. Res. Commun.* **2002**, *294*, 132.
(10) Pinter, T. B. J.; Dodd, E. L.; Bohle, D. S.; Stillman, M. J. *Inorg. Chem.* **2012**, *51*, 3743.
(11) Bohle, D. S.; Dodd, E. L. *Inorg. Chem.* **2012**, *51*, 4411.
(12) Shannon, R. D. *Acta Crystallogr., Sect. A* **1976**, *A32*, 751.
(13) Kadish, K. M.; Cornillon, J. L.; Coutsolelos, A.; Guilard, R. *Inorg. Chem.* **1987**, *26*, 4167.
(14) Kadish, K. M.; Boisselier-Cocolios, B.; Coutsolelos, A.; Mitaine, P.; Guilard, R. *Inorg. Chem.* **1985**, *24*, 4521.
(15) Nakae, Y.; Fukusaki, E. I.; Kajiyama, S. I.; Kobayashi, A.; Nakajima, S.; Sakata, I. *J. Photochem. Photobiol., A* **2005**, *172*, 55.
(16) Wojaczynski, J.; Latos-Grazynski, L. *Inorg. Chem.* **1995**, *34*, 1054.
(17) Boukhris, A.; Lecomte, C.; Coutsolelos, A.; Guilard, R. *J. Organomet. Chem.* **1986**, *303*, 151.
(18) Coutsolelos, A.; Guilard, R.; Bayeul, D.; Lecomte, C. *Polyhedron* **1986**, *5*, 1157.
(19) Coutsolelos, A.; Guilard, R.; Boukhris, A.; Lecomte, C. *J. Chem. Soc., Dalton Trans.* **1986**, 1779.
(20) Guilard, R.; Barbe, J. M.; Richard, P.; Petit, P.; Andre, J. J.; Lecomte, C.; Kadish, K. M. *J. Am. Chem. Soc.* **1989**, *111*, 4684.
(21) Wojaczynski, J.; Latos-Grazynski, L.; Olmstead, M. M.; Balch, A. L. *Inorg. Chem.* **1997**, *36*, 4548.
(22) Balch, A. L.; Hart, R. L.; Parkin, S. *Inorg. Chim. Acta* **1993**, *205*, 137.
(23) Balch, A. L.; Noll, B. C.; Reid, S. M.; Zovinka, E. P. *Inorg. Chem.* **1993**, *32*, 2610.
(24) Arasasingham, R. D.; Balch, A. L.; Olmstead, M. M.; Phillips, S. L. *Inorg. Chim. Acta* **1997**, *263*, 161.
(25) Abraham, R. J.; Eivazi, F.; Pearson, H.; Smith, K. M. *J. Chem. Soc., Chem. Commun.* **1976**, 698.
(26) Abraham, R. J.; Barnett, G. H.; Hawkes, G. E.; Smith, K. M. *Tetrahedron* **1976**, *32*, 2949.
(27) Sasaki, S. I.; Mizoguchi, T.; Tamiaki, H. *Bioorg. Med. Chem. Lett.* **2006**, *16*, 1168.
(28) Bohle, D. S.; Kosar, A. D.; Stephens, P. W. *Acta Crystallogr., Sect. D: Biol. Crystallogr.* **2002**, *D58*, 1752.
(29) Hynes, M. J. *J. Chem. Soc., Dalton Trans.* **1993**, 311.
(30) Frisch, M. J. et al. *Gaussian 03W*, Revision-C.02 Version 6; Gaussian Inc.: Pittsburgh, PA, 2003.
(31) Schuchardt, K. L. D., B. T.; Elsethagen, T.; Sun, L.; Gurumoorthi, V.; Chase, J.; Li, J.; Windus, T. L. *J. Chem. Inf. Model.* **2007**, *47*, 1045.
(32) Feller, D. *J. Comput. Chem.* **1996**, *17*, 1571.
(33) Bellemare, M.-J., Ph.D. Thesis, McGill University, Montreal, Quebec, Canada, 2009.
(34) Bohle, D. S.; Helms, J. *Biochem. Biophys. Res. Commun.* **1993**, *193*, 504.
(35) Deacon, G. B.; Phillips, R. J. *Coord. Chem. Rev.* **1980**, *33*, 227.
(36) Leiserowitz, L. *Acta Crystallogr., Sect. B* **1976**, *B32*, 775.
(37) Bohle, D. S.; Conklin, B. J.; Cox, D.; Madsen, S. K.; Paulson, S.; Stephens, P. W.; Yee, G. T. *ACS Symp. Ser.* **1994**, *572*, 497.
(38) Mack, J. A., Y.; Kobayashi, N.; Stillman, M. J. *J. Am. Chem. Soc.* **2005**, *127*, 17697.
(39) Parzuchowski, P. G.; Kampf, J. W.; Rozniecka, E.; Kondratenko, Y.; Malinowska, E.; Meyerhoff, M. E. *Inorg. Chim. Acta* **2003**, *355*, 302.
(40) Dodd, E., Ph.D. Thesis, McGill University, Montreal, Quebec, Canada, 2012.
(41) Hsieh, Y.-Y.; Sheu, Y.-H.; Liu, I. C.; Lin, C.-C.; Chen, J.-H.; Wang, S.-S.; Lin, H.-J. *J. Chem. Crystallogr.* **1996**, *26*, 203.
(42) DiPasquale, A. G.; Mayer, J. M. *J. Am. Chem. Soc.* **2008**, *130*, 1812.
(43) Steinle, E. D.; Schaller, U.; Meyerhoff, M. E. *Anal. Sci.* **1998**, *14*, 79.
(44) Ponomarev, G. V.; Borovkov, V. V.; Sugiura, K.-I.; Sakata, Y.; Shul'ga, A. M. *Tetrahedron Lett.* **1993**, *34*, 2153.
(45) Wynne, K. J. *Inorg. Chem.* **1985**, *24*, 1339.